diversity

MDPI

Article

Two New *Amanita* Species in Section *Amanita* from Thailand

Yuan S. Liu [1,2], Jian-Kui Liu [3], Jaturong Kumla [1,4] and Saisamorn Lumyong [1,4,5,*]

[1] Department of Biology, Faculty of Science, Chiang Mai University, Chiang Mai 50200, Thailand; yuanshuailiu9@gmail.com (Y.S.L.); Jaturong_yai@hotmail.com (J.K.)
[2] Doctor of Philosophy Program in Applied Microbiology (International Program), Faculty of Science, Chiang Mai University, Chiang Mai 50200, Thailand
[3] School of Life Science and Technology, Center for Informational Biology, University of Electronic Science and Technology of China, Chengdu 611731, China; liujiankui@uestc.edu.cn
[4] Research Center of Microbial Diversity and Sustainable Utilization, Chiang Mai University, Chiang Mai 50200, Thailand
[5] Academy of Science, the Royal Society of Thailand, Bangkok 10300, Thailand
* Correspondence: scboi009@gmail.com; Tel.: +66-81881-3658

Abstract: Based on a survey of macro-fungi in northern and northeastern Thailand, nine samples collected in 2020 are identified as *Amanita* and introduced here as two new species, *Amanita kalasinensis* and *A. ravicrocina*. Typical macro- and microscopical characteristics indicate that both of these two species belong to *Amanita* section *Amanita*, but differ from other currently known species. *Amanita kalasinensis* is characterized by having a greyish yellow pileus covering with a conical to granuliform, yellowish white volval remnant; the presence of clamps; and a broadly ellipsoid to ellipsoid basidiospore. *Amanita ravicrocina* is characterized by having a brown to greyish orange pileus covering with a patchy, white volval remnant; a collar-like volval remnant on the stipe; and a subglobose to broadly ellipsoid basidiospore. Multi-gene phylogenetic analysis of partial nuclear rDNA internal transcribed spacer region (ITS), partial nuclear rDNA large subunit region (nrLSU), RNA polymerase II second largest subunit (*RPB*2), partial translation elongation factor 1-alpha (*TEF*1-α), and beta-tubulin gene (*TUB*) also revealed that positions of *A. kalasinensis* and *A. ravicrocina* are well-supported within *A.* section *Amanita*, but form distinct lineages and do not show any close relationship with any species. The detailed morphological features, line-drawing illustration, and comparison with morphological similar taxa are provided.

Keywords: *Amanitaceae*; diversity; multi-gene; taxonomy; two new species

Citation: Liu, Y.S.; Liu, J.-K.; Kumla, J.; Lumyong, S. Two New *Amanita* Species in Section *Amanita* from Thailand. *Diversity* **2022**, *14*, 101. https://doi.org/10.3390/d14020101

Academic Editor: Ipek Kurtboke

Received: 27 December 2021
Accepted: 28 January 2022
Published: 30 January 2022

1. Introduction

Amanita Pers. is a widespread basidiomycetous genus comprising more than 600 species all over the world [1–5]. According to recent studies [3–5], this genus was proposed to be divided into three subgenera and eleven sections [subgenus *Amanita* Pers., containing: section *Amanita* Pers., section *Amarrendiae* (Bougher & T. Lebel) Zhu L. Yang, Y.Y. Cui, Q. Cai & L.P. Tang, section *Caesareae* Singer ex Singer and section *Vaginatae* (Fr.) Quél; subgenus *Amanitina* (E. J. Gilbert) E. J. Gilbert, containing: section *Amidella* (J. E. Gilbert) Konrad & Maubl., section *Arenariae* Zhu L. Yang, Y.Y. Cui & Q. Cai, section *Phalloideae* (Fr.) Quél., section *Roanokenses* Singer ex Singer, section *Strobiliformes* Singer ex Q. Cai, Zhu L. Yang & Y.Y. Cui and section *Validae* (Fr.) Quél., and subgenus *Lepidella* Beauseigneur, containing section *Lepidella* Corner & Bas only]. Species in *Amanita* section *Amanita* are characterized by having agaricoid basidioma, persistent volval remnants on the pileus, striate pileal margins, truncate lamellulae, basal bulb, and inamyloid basidiospores [1–4]. To date, there are thirteen species from *Amanita* sect. *Amanita*, namely, *A.* aff. *mira* Corner & Bas, *A. altipes* Zhu L. Yang, M. Weiß & Oberw., *A. concentrica* T. Oda, C. Tanaka & Tsuda, *A. digitosa* Boonprat. & Parnmen, *A. melleialba* Zhu L. Yang, Qing Cai

& Yang Y. Cui, *A. obsita* Corner & Bas, *A. orientigemmata* Zhu L. Yang & Yoshim. Doi, *A. rubrovolvata* S. Imai, *A. siamensis* Sanmee, Zhu L. Yang, P. Lumyong & Lumyong, *A. sinensis* Zhu L. Yang, *A. subglobosa* Zhu L. Yang, *A. submelleialba* Yuan S. Liu & S. Lumyong, and *A. sychnopyramis* f. *subannulata* Hongo, reported in Thailand [4,6–12].

During the period of macrofungal investigation in the rainy season of 2020, nine interesting specimens were collected from deciduous forests dominated by *Dipterocarpus* and *Shorea* species in northern and northeastern Thailand (Chiang Rai, Kalasin, and Sakon Nakhon Provinces, Thailand). Morphological examination and molecular analyses indicated that these collections herein reported represent two species new to science.

2. Materials and Methods

2.1. Morphological Study

The following information was recorded at the collecting sites: geographic coordinates, forest type, substrate type, and field photographs. Small pieces of tissue from the cap and/or stipe were taken and dried by silica gel to prepare for the molecular material [13], and the remaining specimens were dried at 35–45 °C for at least twelve hours to prepare for the morphological material and later were deposited at the Herbarium of Biology Department (CMUB) and the Herbarium of Sustainable Development of Biological Resources (SDBR), Faculty of Science, Chiang Mai University, Thailand.

Macroscopic characters were described based on field notes and field images. Color codes and names were recorded according to Kornerup and Wanscher [14]. Marginal striations on the pileus were expressed as a proportion of the ratio of striation length to the radius of the pileus (nR). Microscopic features were observed from dried specimens mounted in distilled water, 5% aqueous KOH (*w*/*v*), 1% Congo red (*w*/*v*), and Melzer's reagent under a Leica DM500 microscope to depict all tissues [2,3]. Sections of the pileipellis were cut radial-perpendicularly, and halfway between the center and margin of the pileus, and sections of the stipitipellis were taken from the center of the stipe, along the middle part along the longitudinal axis. For the description of basidiospores, the term [n/m/p] represents that n basidiospores were measured from m basidiomata of p collections. Dimensions for basidiospores are given as (a–) b–c (–d), in which 'b–c' represents a minimum of 90% of the measured and extreme values 'a' and 'd' are given in parentheses whenever necessary. Q denotes the ratio of length divided by width of the basidiospore in the side view, Qm denotes the average Q of n measured basidiospores, and SD is their standard deviation. The results are presented as Q = Qm ± SD. Basidiomata size and spores shape are defined according to Bas [15].

2.2. DNA Extraction, PCR Amplification, and Sequencing

Methods of DNA extraction, PCR amplification, and sequencing protocols were conducted based on previous studies [4,12,16]. Five primer pairs ITS1F/ITS4 [17,18], LR0R/LR5 [19], EF1-983F/EF1-1567R [20], Am-6 F/Am-7 R, and Am-β-tubulin F/Am-β-tubulin R [21] were used to amplify ITS, nrLSU, *TEF*1-*α*, *RPB*2, and *TUB*, respectively. Sequences generated in this study were subjected to BLASTn (http://www.ncbi.nlm.nih.gov (accessed on 15 December 2021)) analysis and submitted to GenBank.

2.3. Phylogenetic Analyses

Detailed information about the sequences retrieved from GenBank and the sequences newly generated in this study was analyzed (Table 1). Sequences of five gene regions were aligned with MAFFT v.7 [22] using the G-INS-i iterative refinement algorithm, and then checked visually and manually optimized using BioEdit v.7.0.9 [23]. Gblocks v. 0.91b [24] was used to check and exclude the ambiguously aligned regions for ITS, based on two options "Allow smaller final blocks" and "Allow gap positions within the final blocks". Maximum likelihood analyses were carried out for each single gene

dataset using the same settings used for concatenated analysis to test potential conflicts among the five genes. Sequence Matrix v.100.0 was applied to combine the five gene fragments for further phylogenetic analysis and the concatenated dataset was deposited in TreeBASE under the number of 29155. Phylogenetic tree inference was performed using both Bayesian inference (BI) and maximum likelihood (ML), as detailed in Dissanayake et al. [25]. The best-fit model of nucleotide substitution was determined for each single gene dataset using MrModeltest v. 2.3 [26] following the default parameters.

Table 1. Species names, voucher numbers, countries, and their respective GenBank accession numbers of the taxa used in this study.

Species Name	Voucher	Country	GenBank Accession Number				
			ITS	nrLSU	*RPB2*	*TEF1-α*	*TUB*
'Amanita austrowellsii'	RET 302-1	USA	MN963578	MN963578	—	—	—
'A. austrowellsii'	RET 576-2	USA	MN963579	MN963579	—	—	—
A. cruzii T	BARONI 8998 (CORT)	Dominican Republic	KC855222	KC855222	—	MH508750	MH485478
A. cruzii	BARONI 9791 (CORT)	Dominican Republic	KC855223	KC855223	—	MH508751	—
A. elata	HKAS 83449	China	MH508334	MH486486	MH485965	MH508763	MH485488
A. frostiana	RET 547-2	USA	KP313581	—	—	—	—
A. frostiana	RET 588-6	USA	KP313583	—	—	—	—
A. kalasinensis	**SDBR-STO-2020-231**	**Thailand**	**OM040561**	**OM040552**	—	—	—
A. kalasinensis T	**CMUB-39966**	**Thailand**	**OM040562**	**OM040553**	**OM066913**	**OM066919**	**OM066925**
A. kalasinensis	**SDBR-STO-2020-253**	**Thailand**	**OM040563**	**OM040554**	**OM066914**	**OM066920**	
A. kalasinensis	**SDBR-STO-2020-303**	**Thailand**	**OM040564**	**OM040555**	—	—	—
A. kalasinensis	**SDBR-STO-2020-398**	**Thailand**	**OM040565**	**OM040556**	—	—	—
A. mira	HKAS 91953	China	MH508437	MH486646	MH486097	—	—
A. pakistanica	RET 317-6	Pakistan	KX365198	KX365199	—	—	—
A. pakistanica	RET 411-7	India	MG991745	MG991814	—	—	—
A. pantherina	HKAS 56702	Czech Republic	MH508487	KR824782	KR824789	KR824825	MH485670
A. pantherina	MB-102863	Germany	MH508488	MH486743	MH486167	MH508976	MH485671
A. parcivolvata	RET 504-5	USA	KP313586	—	—	—	—
A. parcivolvata	RET 511-10	USA	KP313584	—	—	—	—
A. parcivolvata	RET 614-4	USA	MN963585	MN963584	—	—	—
A. parvipantherina	HKAS 54723	China	MH508495	KR824780	KR824802	KR824807	MH485676
A. parvipantherinaa	HKAS 67907	China	MH508498	KR824781	KR824803	KR824808	MH485679
A. pseudopantherina T	HKAS 80007	China	MH508514	MH486777	MH486191	MH509004	MH485698
A. pseudopantherina	HKAS 57611	China	MH508511	MH486774	MH486188	—	MH485695
A. pseudosychnopyramis	HKAS 82293	China	MH508529	MH486790	MH486204	—	MH485712
A. pseudosychnopyramis T	HKAS 87999	China	MH508530	KR824778	KR824790	KR824824	MH485713
A. rubrovolvata	BZ2015-68	Thailand	KY747465	KY747477	KY656882	—	KY656863
A. rubrovolvata	HKAS 54491	China	JN943178	JN941153	JQ031116	KR824823	—
A. rufoferruginea	HKAS 101395	China	MH508578	MH486839	MH486249	—	MH485753
A. rufoferruginea	HKAS 79616	China	MH508579	MH486842	MH486252	—	MH485756
A. siamensis	HKAS 67855	China	MH508592	MH486864	MH486271	—	MH485773
A. siamensis	HKAS 83681	China	MH508593	MH486866	MH486273	—	MH485774
A. sinensis var. *sinensis* T	HKAS 25761	China	AB096059	AF024474	—	—	AB095864
A. sinensis var. *sinensis*	HKAS 100492	China	MH508594	MH486867	MH486274	—	MH485775
A. sinensis var. *sinensis*	HKAS 100493	China	MH508595	MH486868	MH486275	—	MH485776
A. subglobosa	HKAS 54787	China	MH508618	MH486900	MH486301	MH509121	MH485801
A. subglobosa	HKAS 56893	China	JN943176	JN941157	JQ031120	KR824826	MH485802
A. submelleialba T	CMUB-S1	Thailand	MZ045688	MZ045693	MZ048619	MZ048624	MZ048629
A. submelleialba	HKAS 112958	Thailand	MZ045685	MZ045690	MZ048616	MZ048621	MZ048626
A. submelleialba	HKAS 112959	Thailand	MZ045686	MZ045691	MZ048617	MZ048622	MZ048627
A. subparvipantherina	HKAS 56817	China	JN943171	JN941160	JQ031114	KR824815	MH485818
A. subparvipantherina	HKAS 58891	China	MH508628	MH486918	MH486316	MH509136	MH485819
A. sychnopyramis f. *subannulata*	HKAS 101427	China	MH508631	MH486922	—	MH509139	MH485824
A. sychnopyramis f. *subannulata*	HKAS 101437	China	MH508632	MH486923	MH486319	MH509140	MH485825
A. sychnopyramis f. *subannulata*	HKAS 101442	China	MH508633	MH486925	MH486321	MH509142	MH485826
A. sychnopyramis f. *subannulata*	HKAS 75485	China	MH508634	MH486926	—	MH509143	MH485827
A. wellsii	RET 387-5	Canada	KU248115	OK285332	—	—	—
A. wellsii	RET 654-2	USA	OK299151	OK299151	—	—	—
A. wellsii	RET 726-6	USA	OK299169	OK299169	—	—	—
A. ravicrocina	**SDBR-STO-2020-229**	**Thailand**	**OM040566**	**OM040557**	**OM066915**	**OM066921**	**OM066926**

A. ravicrocina	**SDBR-STO-2020-235**	**Thailand**	**OM040567**	**OM040558**	**OM066916**	**OM066922**	**OM066927**
A. ravicrocina **T**	**CMUB-39967**	**Thailand**	**OM040568**	**OM040559**	**OM066917**	**OM066923**	—
A. ravicrocina	**SDBR-STO-2020-283**	**Thailand**	**OM040569**	**OM040560**	**OM066918**	**OM066924**	—
Outgroup							
A. caesareoides	HKAS 92009	China	MH508285	MH486421	MH485901	MH508708	—
A. caesareoides	HKAS 92017	China	MH508286	MH486422	MH485902	MH508709	—
A. yuaniana	HKAS 58807	China	MH508653	MH486954	MH486347	MH509174	MH485852
A. yuaniana	HKAS 68662	China	MH508654	MH486957	MH486350	MH509177	MH485854

Newly generated sequences in this study are in black bold, while holotypes are marked with "T".

The ML analysis was performed at the CIPRES web portal [27] using RAxML v.8.2.12 as part of the "RAxML-HPC BlackBox" tool [28] with default settings, except the "Estimate proportion of invariable sites (GTRGAMMA+I)" was set to be "yes" for both single-gene and combined gene analyses. Phylogenetic inference was first performed on each single-gene alignment, and as there was no evident conflict (with ML bootstrap support ≥75%), then multiple-gene alignments and trees were built. The Bayesian analysis was performed using MrBayes v.3.1.2 [29]. Posterior probabilities [30] were determined by Markov chain Monte Carlo sampling (MCMC) [31] in MrBayes v.3.1.2. Six simultaneous Markov chains were run from random trees for 1 million generations and trees were sampled every 100th generation (the critical value for the topological convergence diagnostic is 0.01). The first 25% of trees were discarded and the remaining trees were used for calculating posterior probabilities in the majority rule consensus tree. The phylogenetic tree was visualized with FigTree v.1.4.4 [32].

3. Results

3.1. Phylogenetic Analyses

The best-fit models for the five genes were as follows: general time reversible + proportion of invariable sites + gamma distribution (GTR + I + G) for ITS, nrLSU, and *TEF*1-*α*; Hasegawa-Kishino-Yano (HKY) + I + G for *RPB*2; and Kimura 2-parameter (K80) + G for *TUB*. The concatenated dataset was partitioned into five parts by sequence region. The model HKY + I + G and K80 + G could not be implemented in RAxML, thus the GTR + I + G model, which included all parameters of the selected model, was used instead.

The multi-gene dataset comprised 212 sequences, including 33 newly generated and 179 retrieved from GenBank. *Amanita yuaniana* (HKAS58807), *A. yuaniana* (HKAS68662), *A. caesareoides* (HKAS92009), and *A. caesareoides* (HKAS92017) from *Amanita* section *Caesarea* were set as the outgroup taxa. The concatenated dataset comprised 2769 positions (ITS: 1–445; nrLSU: 446–1343; *RPB*2: 1344–2014; *TEF*1-*α*: 2015–2576; and *TUB*: 2577–2803) after alignment, including the gaps.

Bayesian and RAxML analysis of the combined dataset resulted in phylogenetic reconstructions with largely similar topologies, thus the result of maximum likelihood (RAxML) tree is shown in Figure 1. In our phylogenetic results, five collections representing *Amanita kalasinensis* and four collections representing *A. ravicrocina*, respectively, formed a monophyletic lineage from other extant species with credible support values, which could be recognized as two new species.

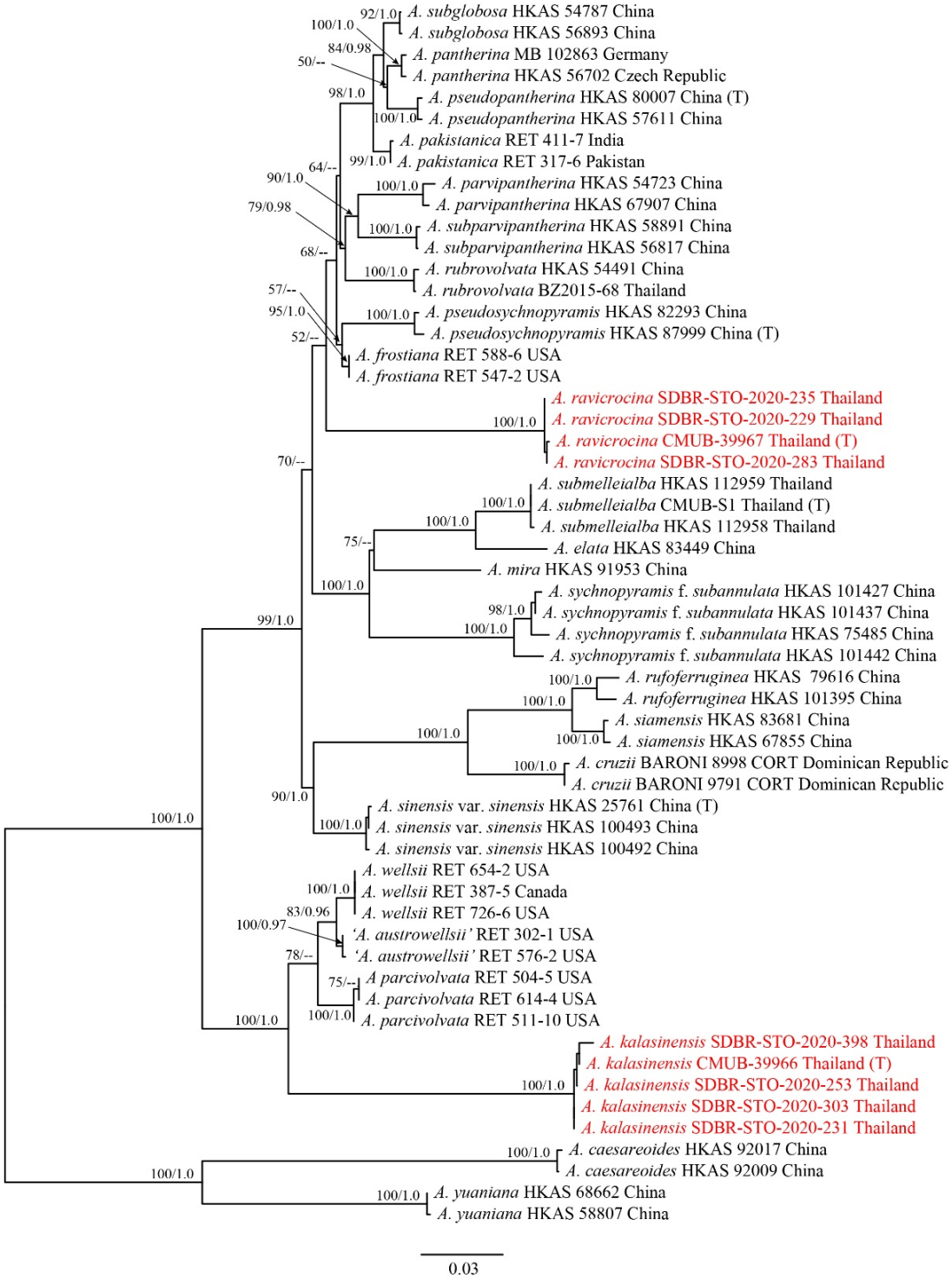

Figure 1. RAxML tree based on a combined of ITS + nrLSU + *RPB*2 + *TEF*1-*α* + *TUB* dataset. Bootstrap values (BS) for ML ≥50% and posterior probabilities (PP) for BI ≥0.95 are placed above or below the branches, respectively. Newly generated sequences are indicated in red and sequences from type material are marked with (T). The tree is rooted with *Amanita yuaniana* (HKAS58807 and HKAS68662) and *A. caesareoides* (HKAS92009 and HKAS92017).

3.2. Taxonomy

Amanita kalasinensis Yuan S. Liu & S. Lumyong, sp. nov. (Figures 2 and 3)
Mycobank number: 842342

Holotype: Thailand, Kalasin Province: Kham Muang District, Na Bon, 16°53′05″ N, 103°41′49″ E, alt. 239 m, 12 August 2020, Yuan S. Liu, STO-2020-233 (CMUB-39966).

Etymology: The specific epithet '*kalasinensis*' refers to the Kalasin province of Thailand, where the holotype was collected.

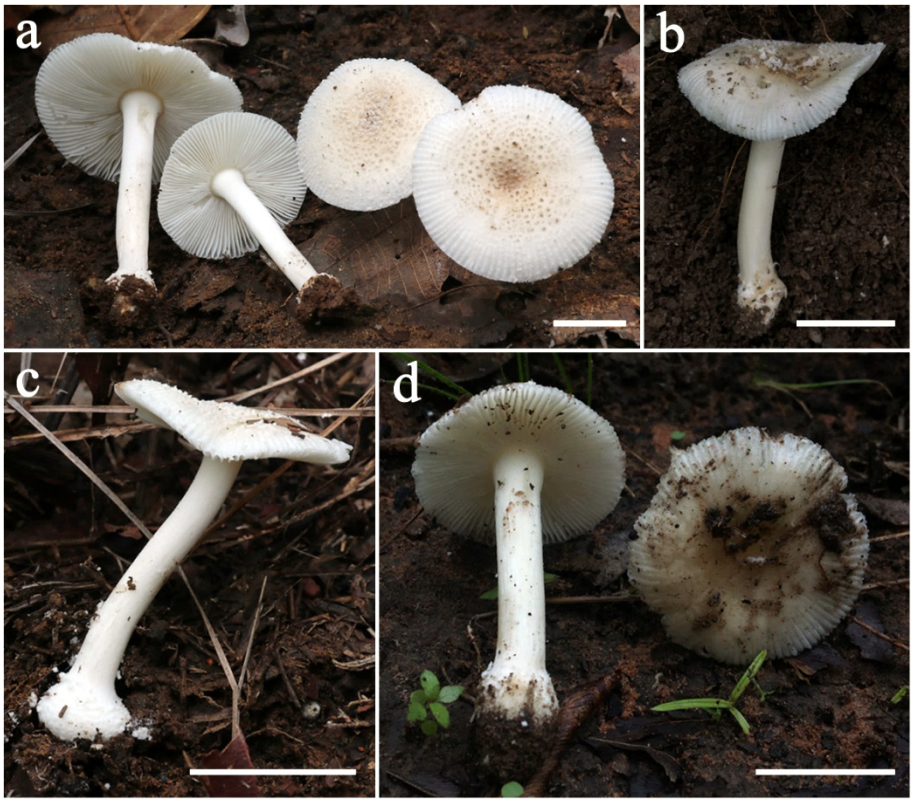

Figure 2. Different collections of Amanita kalasinensis shown in the field. (**a**) CMUB-39966 (holotype). (**b**) SDBR-STO-2020-231. (**c**) SDBR-STO-2020-303. (**d**) SDBR-STO-2020-398. Scale bars: (**a**–**d**) 2 cm.

Description: *Basidioma* small to medium-sized. *Pileus* 3.0–5.7 cm diam., convex, plano-convex to applanate, slightly depressed at center, white (1A1) to greyish yellow (4B3–5), often darker at center and becoming paler towards margin; volval remnants on pileus conical, pyramidal to granuliform, 1–2 mm dia., white (1A1) to yellowish white (4A2), densely arranged on the disk; margin striate (ca. 0.3–0.5), non-appendiculate; context white, unchanging. *Lamellae* free, crowded, white (1A1); lamellulae truncate, plentiful. *Stipe* 3.5–8.0 cm long × 0.6–0.9 cm diam., subcylindrical and slightly tapering upward, with apex slightly expanded, white (1A1) to yellowish white (4A2), sometimes with greyish yellow (4B3–4) tinge, covered with white (1A1) fibrils, often becoming floccose near basal bulb; context white (1A1), stuffed; basal bulb globose to subglobose, 0.9–1.4 cm diam., white (1A1); volval remnants on stipe base granuliform to floccos, white (1A1) to light yellow (4B4–5). *Annulus* absent. *Odor* not recorded.

Lamellar trama bilateral. Mediostratum 15–20 μm wide, composed of abundant clavate to cylindrical inflated cells (54–145 × 13–30 μm); filamentous hyphae abundant, 4–12 μm wide; vascular hyphae scarce. Lateral stratum composed of abundant ellipsoid to clavate inflated cells (32–66 × 13–37 μm), diverging at an angle of ca. 30° to 45° to mediostratum; filamentous hyphae abundant to very abundant, 3–10 μm wide. *Subhymenium* 20–30 μm thick, with 2–3 layers of globose, ellipsoid, or irregular inflated cells, 6–24 × 6–18 μm. *Basidia* (Figure 3b) 37–52 × 12–16 μm, clavate, four-spored; sterigmata 4–6 μm long; basal septa clamped. *Basidiospores* (Figure 3a) [100/3/3] (8.5–) 9.0–11.5 (–13.0) × (6.0–) 7.0–8.5 (–10.0) μm, avl X avw = 10.3 × 7.4 μm, Q = (1.19–) 1.25–1.53 (–1.67) μm, Qm = 1.40 ± 0.09, broadly ellipsoid to ellipsoid, inamyloid, colorless, thin-walled, smooth; apiculus

short but wide, width up to 1.5 μm. *Lamellar edge* appearing as a sterile strip, composed of very abundant to nearly dominant globose, subglobose, ellipsoid, or irregular inflated cells (11–26 × 8–25 μm), single and terminal or in chains of 2–3, thin-walled, colorless; filamentous hyphae scattered, 3–6 μm wide, irregularly arranged or parallel to lamellar edge. *Pileipellis* 130–205 μm thick, composed of radial, thin-walled, colorless, filamentous hyphae 3–17 μm wide; vascular hyphae scarce. *Volval remnants* on pileus (Figure 3c) composed of vertically to subvertically arranged elements: filamentous hyphae fairly abundant to abundant, 2–8 μm wide, colorless, thin-walled, branching, anastomosing; inflated cells abundant, globose, subglobose, to ellipsoid, sometimes irregular, 23–65 × 15–55 μm, colorless, thin-walled, terminal or in chains of 2–3; vascular hyphae scarce. *Volval remnants* on stipe base is semblable with the structure of volval remnants on pileus, composed of irregularly arranged elements: filamentous hyphae very abundant to nearly dominant, 2–11 (–15) μm wide, colorless, thin-walled, branching, anastomosing; inflated cells fairly abundant, globose, subglobose to ellipsoid, sometimes irregular, 12–88 × 10–55 μm, colorless, thin-walled; vascular hyphae scarce. *Stipe trama* composed of longitudinally arranged, clavate terminal cells, 90–265 × 20–48 μm; filamentous hyphae abundant, 2–16 μm wide; vascular hyphae scarce. *Clamps* present in all parts of basidioma.

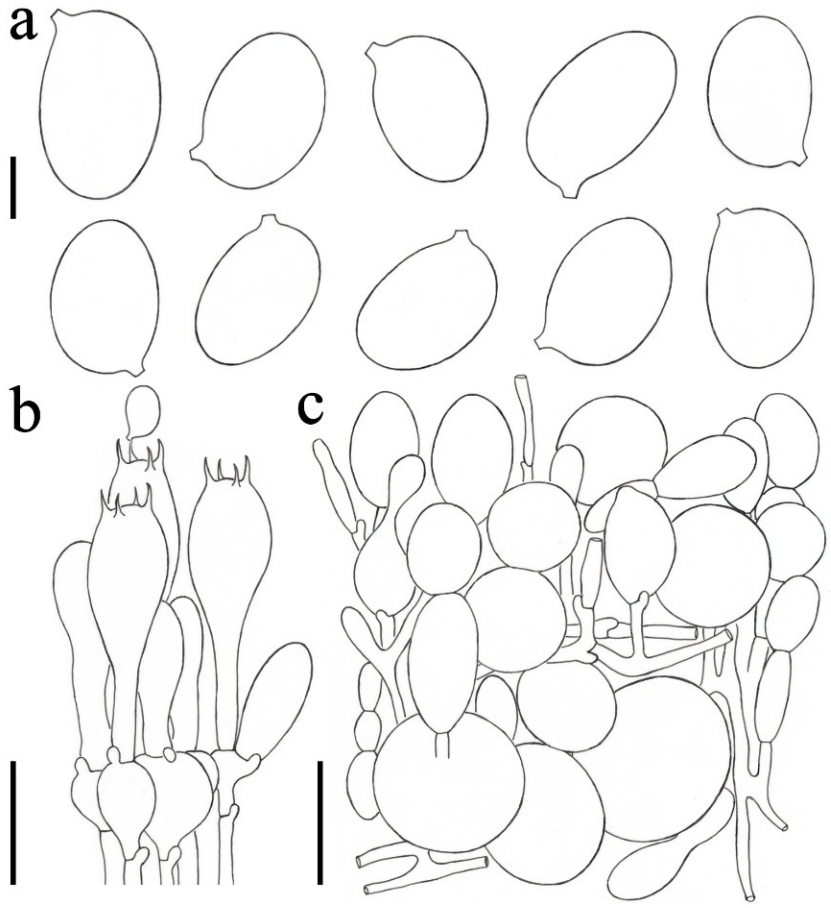

Figure 3. *Amanita kalasinensis* (CMUB-39966, holotype). (**a**) Basidiospores. (**b**) Hymenium and subhymenium. (**c**) Longitudinal section of volval remnants on pileus. Bars: (**a**) 4 μm; (**b**) 20 μm; (**c**) 40 μm.

Habitat: Solitary to scattered on soil in tropical deciduous forests dominant by *Dipterocarpus* and *Shorea*. Basidioma occurs in the rainy season during May to October.

Distribution: Currently known from northern and northeastern Thailand

Additional collections examined: Thailand, Kalasin Province: Kham Muang District, Na Bon, 16°53′05″ N, 103°41′49″ E, alt. 239 m, 12 August 2020, Yuan S. Liu, STO-2020-231

(SDBR-STO-2020-231); Kalasin Province: Somdet District, Mahachai, 16°48′38″ N, 103°46′13″ E, alt. 197 m, 14 August 2020, Yuan S. Liu, STO-2020-253 (SDBR-STO-2020-253); Sakon Nakhon Province: Kut Bak District, Na Mong, 17°06′04″ N, 103°54′32″ E, alt. 208 m, 15 August 2020, Yuan S. Liu, STO-2020-303 (SDBR-STO-2020-303); Chiang Mai Province: Mueang Chiang Mai District, Suthep, 18°48′10″ N, 98°57′02″ E, alt. 343 m, 26 August 2020, Yuan S. Liu, STO-2020-398 (SDBR-STO-2020-398).

Notes: *Amanita kalasinensis* is similar to several species that have a light yellow tinge pileus covered by pyramidal to granuliform, white volva remnants, such as *A. parvipantherina* Zhu L. Yang, M. Weiß & Oberw., *A. sychnophyramis* f. *subannulata* Hongo, and *A. sychnophyramis* Corner & Bas f. *sychnopyramis*. However, both *A. parvipantherina* [33,34] and *A. sychnophyramis* f. *subannulata* [1–3,35] differ from *A. kalasinensis* by having a white or brownish annulus on its stipe, as well as a darker brownish pileus.. *Amanita sychnophyramis* f. *sychnophyramis*, occurring in Singapore, China, and Malaysia [3,36,37], is discerned from *A. kalasinensis* by having a larger and darker brownish pileus. Furthermore, compared with the former species, which is short of clamp and has a globose to subglobose basidiospore (6.5–8.5 × 6–8 μm, Q = 1.01–1.11, Qm = 1.06 ± 0.03), *A. kalasinensis* has obvious clamps and a broadly ellipsoid to ellipsoid basidiospore (9.0–11.5 × 7.0–8.5 μm, Q = 1.25–1.53 μm, Qm = 1.40 ± 0.09).

Amanita ravicrocina Yuan S. Liu & S. Lumyong sp. nov. (Figures 4 and 5)

Mycobank number: 842343

Holotype: Thailand. Sakon Nakhon Province: Phu Phan District, Khok Phu, 17°00′09″ N, 103°57′34″ E, alt. 291 m, 15 August 2020, Yuan S. Liu, STO-2020-282 (CMUB-39967).

Etymology: *ravicrocina*, from ravus = greyish, and crocinus = orange, refers to its greyish orange pileus.

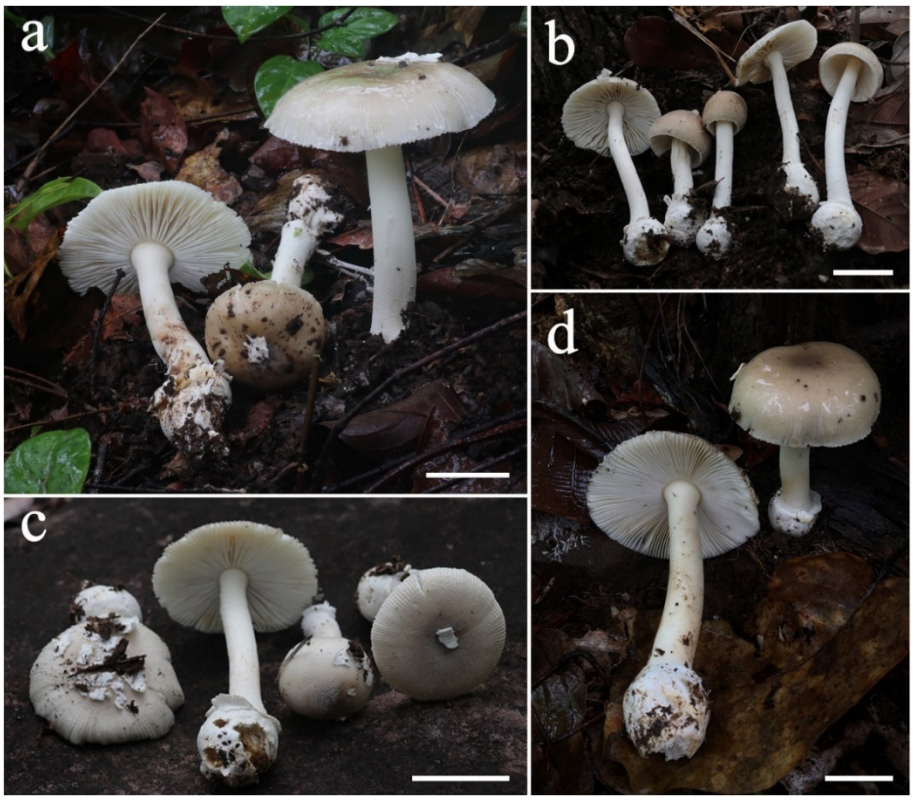

Figure 4. Different collections of *Amanita ravicrocina* shown in the field. (**a**) CMUB-39967 (holotype). (**b**) SDBR-STO-2020-235. (**c**) SDBR-STO-2020-229. (**d**) SDBR-STO-2020-283. Scale bars: (**a**–**d**) 3 cm.

Description: *Basidioma* small to medium-sized. *Pileus* 3.0–8.5 cm diam., convex to plano-convex, often slightly depressed at center, brown (5E5), greyish orange (5B4–5) to

orange white (5A2), often darker at center and becoming paler towards margin; volval remnants on pileus often persistent as large, thick, white (1A1) patches slightly attached on pileus; margin striate (ca. 0.3–0.5), non-appendiculate; context white, unchanging. *Lamellae* free, crowded, white (1A1); lamellulae truncate. Stipe 5.6–13.1 cm long × 0.8–1.4 cm diam., slender, subcylindrical and slightly tapering upward, with apex slightly expanded, white (1A1), covered with white (1A1) fibrils, becoming floccose near basal bulb; context white (1A1), fistulose; basal bulb globose to subglobose, 1.8–2.9 cm diam., white (1A1); volval remnants on stipe base formed a collar-like or shortly limbate volva on limit between stipe and basal bulb, white (1A1). *Annulus* absent. *Odor* not recorded.

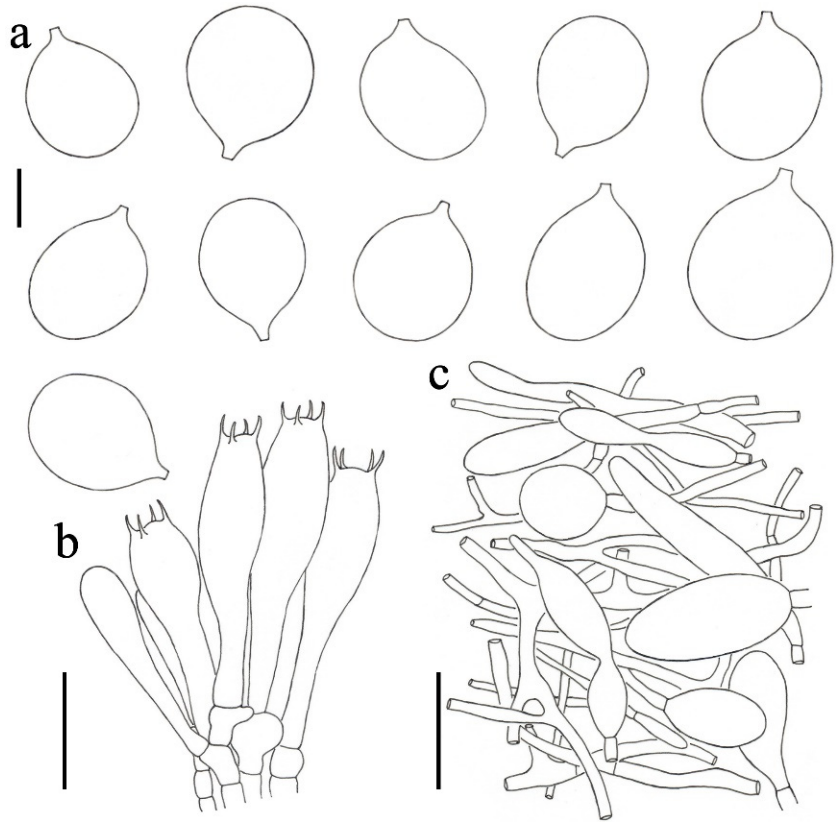

Figure 5. *Amanita ravicrocina* (CMUB-39967, holotype). (**a**) Basidiospores. (**b**) Hymenium and subhymenium. (**c**) Longitudinal section of volval remnants on pileus. Bars: (**a**) 4 μm; (**b**) 20 μm; (**c**) 40 μm.

Lamellar trama bilateral. Mediostratum 15–30 μm wide, composed of abundant clavate to cylindrical inflated cells (25–160 × 12–35 μm); filamentous hyphae abundant, 2–7 μm wide; vascular hyphae scarce. Lateral stratum composed of abundant ellipsoid to clavate inflated cells (50–155 × 7–18 μm), diverging at an angle of ca. 30° to 45° to mediostratum; filamentous hyphae abundant, 2–8 μm wide. *Subhymenium* 20–30 μm thick, with 2–3 layers of subglobose, pyriform, or irregular cells, 8–19 × 5–10 μm. *Basidia* (Figure 5b) 38–52 × 10–14 μm, clavate, four-spored; sterigmata 3–6 μm long; basal septa lacking clamps. *Basidiospores* (Figure 5a) [100/5/4] (7.0–) 8.0–9.5 (–10.5) × (6.0–) 7.0–8.5 (–9.0) μm, avl X avw = 8.7 × 7.5 μm, Q = (1.00–) 1.06–1.29 (–1.36) μm, Qm = 1.16 ± 0.08, subglobose to broadly ellipsoid, inamyloid, colorless, thin-walled, smooth; apiculus small. *Lamellar edge* appearing as a sterile strip, composed of abundant subglobose to ellipsoid inflated cells (8–25 × 6–12 μm), single and terminal or in chains of 2–3, thin-walled, colorless; filamentous hyphae fairly abundant, 2–8 μm wide, irregularly arranged or parallel to lamellar edge. *Pileipellis* 60–100 μm thick, composed of radial, thin-walled, colorless, filamentous hyphae 2–10 μm wide; vascular hyphae scarce. *Volval remnants* on pileus (Figure 5c) composed of irregularly arranged elements: filamentous hyphae abundant to very

abundant, 2–10 μm wide, colorless, thin-walled, branching, anastomosing; inflated cells abundant, globose, subglobose, fusiform to ellipsoid, sometimes irregular, 20–90 × 14–46 μm, colorless, thin-walled, terminal or in chains of 2–4; vascular hyphae scarce. *Volval remnants* on stipe base is semblable with the structure of volval remnants on pileus, composed of irregularly arranged elements: filamentous hyphae very abundant to nearly dominant, 2–9 (–12) μm wide, colorless, thin-walled, branching, anastomosing; inflated cells fairly abundant to abundant, globose, subglobose, ellipsoid to clavate, sometimes irregular, 18–90 × 11–35 μm, colorless, thin-walled; vascular hyphae scarce. *Stipe trama* composed of longitudinally arranged, clavate terminal cells, 75–235 × 18–36 μm; filamentous hyphae abundant, 3–11 μm wide; vascular hyphae scarce. *Clamps* absent in all parts of basidioma.

Habitat: Solitary to scattered on soil in tropical deciduous forests dominant by *Dipterocarpus* and *Shorea*. Basidioma occurs in the rainy season during May to October.

Distribution: Currently known from northeastern Thailand.

Additional collections examined: Thailand, Kalasin Province: Kham Muang District, Na Bon, 16°53′05″ N, 103°41′49″ E, alt. 239 m, 12 August 2020, Yuan S. Liu, STO-2020-229 (SDBR-STO-2020-229); Yuan S. Liu, STO-2020-235 (SDBR-STO-2020-235); Sakon Nakhon Province: Phu Phan District, Khok Phu, 17°00′09″ N, 103°57′34″ E, alt. 291 m, 15 August 2020, Yuan S. Liu, STO-2020-283 (SDBR-STO-2020-283).

Notes: *Amanita ravicrocina* has a collar-like volva remnant on the limit between stipe and inflated basal bulb, which is not a common characteristic in *A.* section *Amanita*. Coupled with a brown tone pileus surface, *A. ravicrocina* could be easily singled out from other species in *A.* section *Amanita*, except *A. ibotengutake* T. Oda, C. Tanaka & Tsuda, *A. pseudopantherina* Zhu L. Yang ex Yang-Yang Cui, Qing Cai & Zhu L. Yang, and *A. subglobosa* Zhu L. Yang. Nevertheless, the latter three taxa are distinguished from *A. ravicrocina* by having the membranous annulus and pyramidal to subconical volva remnants on pileus [1,4,38]. In addition, *A. parvipantherina* [4,33] also possesses close likeness with *A. ravicrocina*. Both of them have small to medium-sized basidiomata and a light grey to brown pileus surface. However, *A. parvipantherina* has a white to brownish annulus, and its volva remnants on pileus are verrucose to pyramidal, while *A. ravicrocina* has a short annulus and appears as patchy volva remnants on pileus.

4. Discussion

As mentioned above, thirteen species in section *Amanita* have been described in Thailand. Although most of these species are based on both of morphologic and phylogenetic evidences, four species, namely, *A.* aff. *mira*, *A. obsita*, *A. siamensis*, and *A. subglobosa*, have only morphologic data [6], which need to be supplemented with more molecular data to confirm their taxonomic status. Our study, along with other previous studies, allowed to discover the high diversity of *Amanita* species in Thailand [6–12], indicating that more taxa remain to be discovered and documented.

In our multi-gene phylogenetic analyses, both *Amanita kalasinensis* and *A. ravicrocina* formed a well-supported (BS = 100%, PP = 1.0) monotypic clade. However, the position of *A. ravicrocina* is not stable. Despite that many potential causes could lead to these unstable topologies, the primary reason might be that *A. ravicrocina* has significant differences from any other existing *Amanita* species in each single gene (the highest similarity and its query cover of initial BLAST searches results in GenBank for ITS and nrLSU of *A. ravicrocina* samples were from following: *A. frostiana*—RET 588-6 (KP313583) with 89.23% similarity and 99% query cover for ITS, and *A. altipes*—BZ2013-42 (MH716040) with 97.58% similarity and 100% query cover for nrLSU).

The erratic positions of *Amanita ravicrocina* and its distinct sequences provide indirect evidence that there are probably some new taxa related to *A. ravicrocina* that remain to be discovered. Therefore, further exploration of *Amanita* diversity is critical, which could reveal more members in this section.

Author Contributions: Conceptualization, Y.S.L. and S.L.; methodology, Y.S.L.; formal analysis, Y.S.L.; resources, Y.S.L.; data curation, Y.S.L.; writing—original draft preparation, Y.S.L.; writing—review and editing, J.-K.L., J.K. and S.L.; supervision, J.-K.L. and S.L.; project administration, S.L.; funding acquisition, S.L. All authors have read and agreed to the published version of the manuscript.

Funding: This study was supported by TA&RA Scholarship, graduate school, Chiang Mai University, and partially supported by Chiang Mai University, Thailand.

Institutional Review Board Statement: Not applicable.

Data Availability Statement: The DNA sequences data obtained from this study were deposited in GenBank under accession numbers: ITS (OM040561, OM040562, OM040563, OM040564, OM040565, OM040566, OM040567, OM040568, OM040569), nrLSU (OM040552, OM040553, OM040554, OM040555, OM040556, OM040557, OM040558, OM040559, OM040560), *RPB2* (OM066913, OM066914, OM066915, OM066916, OM066917, OM066918), *TEF*1-α (OM066919, OM066920, OM066921, OM066922, OM066923, OM066924), and *TUB* (OM066925, OM066926, OM066927).

Acknowledgments: We are very grateful to Zhu-Liang Yang for his guidance in microscopic features observation and drawing. We also appreciate Jean Evans I. Codjia for his valuable suggestions.

Conflicts of Interest: The authors declare no conflict of interest.

References

1. Yang, Z.L. Die *Amanita*-Arten von Südwestchina. *Bibl. Mycol.* **1997**, *170*, 1–240.
2. Yang, Z.L. *Amanitaceae. Flora Fungorum Sinicorum 27*; Science Press: Beijing, China, 2005; pp. 1–258.
3. Yang, Z.L. *Atlas of the Chinese Species of Amanitaceae*; Science Press: Beijing, China, 2015; pp. 1–213.
4. Cui, Y.Y.; Cai, Q.; Tang, L.P.; Liu, J.W.; Yang, Z.L. The family Amanitaceae: Molecular phylogeny, higher-rank taxonomy and the species in China. *Fungal Divers.* **2018**, *91*, 5–230.
5. Amanitaceae org. Available online: http://www.amanitaceae.org/?Genus%20*Amanita* (accessed on 5 December 2021).
6. Sanmee, R.; Tulloss, R.E.; Lumyong, P.; Dell, B.; Lumyong, S. Studies on *Amanita* (*Basidiomycetes*: *Amanitaceae*) in Northern Thailand. *Fungal Divers.* **2008**, *3*, 97–123.
7. Li, G.J.; Hyde, K.D.; Zhao, R.L.; Hongsanan, S.; Abdel-Aziz, F.A.; AbdelWahab, M.A.; Alvarado, P.; Alves-Silva, G.; Ammirati, S.F.; Ariyawansa, H.A.; et al. Fungal diversity notes 253–366: Taxonomic and phylogenetic contributions to fungal taxa. *Fungal Divers.* **2016**, *78*, 1–237.
8. Thongbai, B.; Tulloss, R.E.; Miller, S.L.; Hyde, K.D.; Chen, J.; Zhao, R.L.; Raspé, O. A new species and four new records of *Amanita* (*Amanitaceae*; *Basidiomycota*) from Northern Thailand. *Phytotaxa* **2016**, *286*, 211–231.
9. Thongbai, B.; Miller, S.L.; Stadler, M.; Stadler, M.; Wittstein, K.; Hyde, K.D.; Lumyong, S.; Raspé, O. Study of three interesting *Amanita* species from Thailand: Morphology, multiple-gene phylogeny and toxin analysis. *PLoS ONE* **2017**, *12*, e0182131.
10. Thongbai, B.; Hyde, K.D.; Lumyong, S.; Raspé, O. High undescribed diversity of *Amanita* section *Vaginatae* in northern Thailand. *Mycosphere* **2018**, *9*, 462–494.
11. Phookamsak, R.; Hyde, K.D.; Jeewon, R.; Bhat, D.J.; Jones, E.B.G.; Maharachchikumbura, S.S.N.; Raspe, O.; Karunarathna, S.C.; Wanasinghe, D.N.; Hongsanan, S.; et al. Fungal diversity notes 929–1035: Taxonomic and phylogenetic contributions on genera and species of fungi. *Fungal Divers.* **2019**, *95*, 1–273.
12. Liu, Y.S.; Liu, J.K.; Mortimer, P.E.; Lumyong, S.L. *Amanita submellealba* sp. nov. in section *Amanita* from northern Thailand. *Phytotaxa* **2021**, *513*, 129–140.
13. Zhang, L.F.; Yang, Z.L. Recommendation of several methods for preserving the materials of macro fungi for molecular biological research. *J. Fungal Res*. **2004**, *2*, 60–61.
14. Kornerup, A.; Wanscher, J.H. *Methuen Handbook of Colour*, 3rd ed.; Eyre Methuen: London, UK, 1978; pp. 1–243.
15. Bas, C. Morphology and subdivision of Amanita and a monograph of its section Lepidella. *Persoonia* **1969**, *5*, 285–579.
16. Cai, Q.; Cui, Y.Y.; Yang, Z.L. Lethal *Amanita* species in China. *Mycologia* **2016**, *108*, 993–1009.
17. White, T.J.; Bruns, T.; Lee, S.; Taylor, J.W. Amplification and direct sequencing of fungal ribosomal RNA genes for phylogenetics. In *PCR Protocols: A Guide to Methods and Applications*; Innis, M.A., Gelfand, D.H., Sninsky, J.J., White, T.J., Eds.; Academic Press: San Diego, CA, USA, 1990; Volume 38, pp. 315–322.
18. Gardes, M.; Bruns, T.D. ITS primers with enhanced specificity for basidiomycetes application to the identification of mycorrhizae and rusts. *Mol. Ecol.* **1993**, *2*, 113–118.
19. Vilgalys, R.; Hester, M. Rapid genetic identification and mapping of enzymatically amplified ribosomal DNA from several *Cryptococcus* species. *J. Bacteriol*. **1990**, *172*, 4238–4246.
20. Rehner, S.A.; Buckley, E. A Beauveria phylogeny inferred from nuclear ITS and EF1-α sequences: Evidence for cryptic diversification and links to *Cordyceps* teleomorphs. *Mycologia* **2005**, *97*, 84–98.

21. Cai, Q.; Tulloss, R.E.; Tang, L.P.; Tolgor, B.; Zhang, P.; Chen, Z.H.; Yang, Z.L. Multi-locus phylogeny of lethal *amanitas*: Implications for species diversity and historical biogeography. *BMC Evol. Biol.* **2014**, *14*, 143.
22. Katoh, K.; Standley, D.M. MAFFT multiple sequence alignment software version 7: Improvements in performance and usability. *Mol. Biol. Evol*. **2013**, *30*, 772–780.
23. Hall, T.A. BioEdit: A user-friendly biological sequence alignment editor and analysis program for Windows 95/98/NT. *Nucleic Acids Symp. Ser.* **1999**, *41*, 95–98.
24. Castresana, J. Selection of conserved blocks from multiple alignments for their use in phylogenetic analysis. *Mol. Biol. Evol*. **2000**, *17*, 540–552.
25. Dissanayake, A.J.; Bhunjun, C.S.; Maharachchikumbura, S.S.N.; Liu, J.K. Applied aspects of methods to infer phylogenetic relationships amongst fungi. *Mycosphere* **2020**, *11*, 2652–2676.
26. Nylander, J.A.A. *MrModeltest v2. Program Distributed by the Author*; Evolutionary Biology Centre, Uppsala University: Uppsala, Sweden, 2004.
27. Miller, M.A.; Pfeiffer, W.; Schwartz, T. Creating the CIPRES Science Gateway for Inference of Large Phylogenetic Trees. In Proceedings of the Gateway Computing Environments Workshop, New Orleans, LA, USA, 14 November 2010; pp. 1–8.
28. Stamatakis, A. RAxML Version 8: A tool for Phylogenetic Analysis and Post-Analysis of Large Phylogenies. *Bioinformatics* **2014**, *30*, 1312–1313.
29. Ronquist, F.; Huelsenbeck, J.P. MrBayes3: Bayesian phylogenetic inference under mixed models. *Bioinformatics* **2003**, *19*, 1572–1574.
30. Rannala, B.; Yang, Z. Probability distribution of molecular evolutionary trees: A new method of phylogenetic inference. *J. Mol. Evol.* **1996**, *43*, 304–311.
31. Larget, B.; Simon, D.L. Markov chain Monte Carlo algorithms for the Bayesian analysis of phylogenetic trees. *Mol. Biol. Evol.* **1999**, *16*, 750–759.
32. FigTree v1.4.4. Available online: http://tree.bio.ed.ac.uk/software/figtree/ (accessed on 25 November 2021).
33. Yang, Z.L.; Weiß, M.; Oberwinkler, F. New species of *Amanita* from the Eastern Himalaya and adjacent regions. *Mycologia* **2004**, *96*, 636–646.
34. Bhatt, R.P.; Mehmood, T.; Uniyal, P.; Singh, U. Six new records of genus *Amanita* (*Amanitaceae*) from Uttarakhand, India. *Curr. Res. Environ. Appl. Mycol*. **2017**, *7*, 161–182.
35. Hongo, T. Notulae Mycologicae (10). *Mem. Shiga Univ*. **1971**, *21*, 62–68.
36. Corner, E.J.H.; Bas, C. The genus *Amanita* in Singapore and Malaya. *Persoonia* **1962**, *2*, 241–304.
37. Lee, S.S. *A Field Guide to the Larger Fungi of FRIM*; Forest Research Institute Malaysia: Kuala Lumpur, Malaysia, 2017; pp. 1–174.
38. Oda, T.; Yamazaki, T.; Tanaka, C.; Terashita, T.; Taniguchi, N.; Tsuda, M. *Amanita ibotengutake* sp. nov., a poisonous fungus from Japan. *Mycol. Prog*. **2002**, *1*, 355–365.